Structure of Protein Tyrosine Phosphatase 1B in Complex with Inhibitors Bearing Two Phosphotyrosine Mimetics

Zongchao Jia,[†] Qilu Ye,[†] A. Nicole Dinaut,[‡] Qingping Wang,[§] Deena Waddleton,[§] Paul Payette,[§] Chidambaram Ramachandran,[§] Brian Kennedy,[§] Gabriel Hum,[‡] and Scott D. Taylor*[,‡]

Department of Chemistry, University of Waterloo, Waterloo, Ontario, N2L 3G1, Canada, Department of Biochemistry, Queen's University, Kingston, Ontario, K7L 3N6, Canada, and Department of Biochemistry and Molecular Biology, Merck-Frosst Center for Therapeutic Research, Pointe-Claire, Dorval, Quebec, H9R 4P8, Canada

Received June 14, 2001

Protein tyrosine phosphatases (PTPases) are signal-transducing enzymes that dephosphorylate intracellular proteins that have phosphorylated tyrosine residues. It has been demonstrated that protein tyrosine phosphatase 1B (PTP1B) is an attractive therapeutic target because of its involvement in regulating insulin sensitivity (Elcheby et al. *Science* **1999**, *283*, 1544−1548). The identification of a second binding site in PTP1B (Puius et al. , *Proc. Natl. Acad. Sci. U.S.A.* **1997**, 94, 13420−13425) suggests a new strategy for inhibitor design, where appropriate compounds may be made to simultaneously occupy both binding sites to gain much higher affinity and selectivity. To test this hypothesis and gain further insights into the structural basis of inhibitor binding, we have determined the crystal structure of PTP1B complexed with two non-peptidyl inhibitors, **4** and **5**, both of which contain two aryl difluoromethylenephosphonic acid groups, a nonhydrolyzable phosphate mimetic. The structures were determined and refined to 2.35 and 2.50 Å resolution, respectively. Although one of the inhibitors seems to have satisfied the perceived requirement for dual binding, it did not bind both the active site and the adjacent noncatalytic binding site as expected. The second or distal phosphonate group instead extends into the solvent and makes water-mediated interactions with Arg-47. The selectivity of the more potent of these two inhibitors, as well as four other inhibitors bearing two such phosphate mimetics for PTP1B versus seven other PTPases, was examined. In general, selectivity was modest to good when compared to PTPases Cdc25a, PTPmeg-1, PTPβ, and CD45. However, selectivity was generally poor when compared to other PTPases such as SHP-1, SHP-2, and especially TCPTP, for which almost no selectivity was found. The implications these results have concerning the utility of dual-binding inhibitors are discussed.

Protein tyrosine phosphatases (PTPases) are signal-transducing enzymes that dephosphorylate intracellular proteins phosphorylated at tyrosine residues. Together with protein tyrosine kinases, which catalyze the opposing protein phosphorylation reactions, protein tyrosine phosphatases regulate the level and extent of protein tyrosine phosphorylation and play vital roles in regulating many and diverse cellular processes. These include cell growth, proliferation and differentiation, metabolism, immune responses, cell−cell adhesion, and cell−matrix contacts.[1−5]

Protein tyrosine phosphatases are classified as intracellular PTPases or receptor-like PTPases depending on the cellular localization of these enzymes.[1−5] Among PTPs, human protein tyrosine phosphatase 1B (PTP1B) has been the most extensively studied. The enzyme is widely expressed in insulin-sensitive tissues and has been implicated in the attenuation of insulin signaling.[6] A recent transgenic experiment has demonstrated that PTP1B plays a key regulatory role in modulating both insulin sensitivity and resistance to diet-induced obesity.[7] Thus, it is being increasingly recognized as a potential therapeutic target for the treatment of type 2 diabetes and obesity. In addition, PTP1B may also be a key regulatory component of other pathways. For example, overexpression of PTP1B has been shown to occur in a significant percentage of breast cancer patients.[8] It has also been demonstrated that PTP1B dephosphorylates $p130^{Cas}$, suggesting that it may have a regulatory role in mitogen-mediated signal transduction pathways.[9] Consequently, there is tremendous interest in obtaining inhibitors of this enzyme.[10,11]

Over the past several years, numerous reports have appeared in the literature describing inhibitors of PTP1B.[11] Although a number of highly potent or selective inhibitors of PTP1B have been prepared, combining both of these features in a single molecule is still problematic. Early attempts to prepare both potent and selective PTP1B inhibitors involved preparing peptidyl structures in which the labile phosphotyrosine (pTyr) residue is replaced with a nonhydrolyzable pTyr mimetic.[10] The most effective of these mimetics was the difluoromethylphosphonic acid (DFMP) group, first utilized by Burke and co-workers.[12,13] Certain peptides bearing difluoromethylphosphonophenylalanine (F_2-Pmp, **1**) exhibited affinities for PTP1B that were more than an order of magnitude greater than the analogous peptide substrates and exhibited some selectivity for PTP1B over other PTPases examined. Later, Moran et

* To whom correspondence should be addressed: phone, (519) 888-4567, ext 3325; fax, (519) 746-0435; e-mail, s5taylor@sciborg.uwaterloo.ca.
[†] Queen's University.
[‡] University of Waterloo.
[§] Merck-Frosst Center for Therapeutic Research.

10.1021/jm010266w CCC: $20.00
Published on Web 11/28/2001

al reported that certain tripeptides bearing a cinnamic acid moiety were potent inhibitors of PTP1B, exhibiting

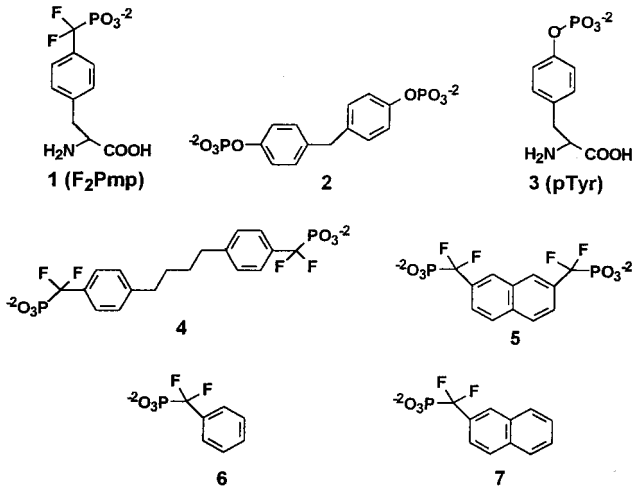

K_i's as low as 79 nM.[14] However, there is some question as to whether these compounds are acting as reversible inhibitors or as irreversible affinity labels. Peptides bearing sulfotyrosine,[15,16] *O*-malonyltyrosine,[17] fluoro-*O*-malonyltyrosine,[18,19] and other pTyr mimetics[20] are also inhibitors of PTP1B though none are as effective phosphate mimetics as the DFMP group. Because of the problems associated with the development of peptide-based therapeutics, more recent efforts have focused on developing small-molecule PTP1B inhibitors. Burke and co-workers[21,22] and later ourselves[23−25] reported that even relatively simple aryl derivatives bearing a single DFMP group were modest inhibitors of PTP1B. Rice et al. have examined a series of triamides functionalized with an isoxazole ring, a carboxylic acid group, and various hydrophobic moieties.[26] One of these compounds was a noncompetitive inhibitor of PTP1B with a K_i of 850 nM. Modest selectivity was found between PTP1B and dual specificity phosphatases Cdc25A, -B, and -C. Its selectivity with other PTPases was not reported. Very recently, researchers at Wyeth-Ayerst reported that certain compounds from a series of benzofuran and benzothiophene derivatives, as well as a series of azolidinediones, were potent inhibitors of PTP1B, exhibiting IC_{50} values in the 11−300 nM range.[27−29] Selectivity for PTP1B over other PTPases varied anywhere from 5- to 175-fold. Also reported very recently was the inhibition of PTP1B with a series of oxalylaminobenzoic acid derivatives.[30,31] The most potent compound from this series exhibited an IC_{50} of 5 μM with PTP1B at physiological pH; however, it was highly selective (>150-fold) for PTP1B compared to other PTPases examined (SHP-1, PTPα D1, PTPϵ D1, PTPβ, CD45 D1D2, LAR D1D2).

In addition to the primary binding pocket or the active site, a second noncatalytic aryl phosphate binding site with lower binding affinity has been identified in PTP1B.[32] The second site was discovered by crystallizing PTP1B in the presence of the high-affinity bis-phosphonate substrate **2** (K_m = 16 μM)[33] or saturating (53 mM) amounts of phosphotyrosine (**3**, pTyr). pTyr was found to bind in two different modes. In one mode (pTyr A), the phosphate group of pTyr binds in the catalytic site in the usual manner. In the other mode (pTyr B), the phosphate group binds by forming ionic interactions with Arg-254 and Arg-24 and water-mediated hydrogen bonds with Met-258 and Gly-259. Although with saturating pTyr both sites could be occupied simultaneously, only 50% of the pTyr was bound as pTyrB. These results suggest that PTP1B contains one high-affinity catalytic aryl phosphate binding site and, adjacent to it, one low-affinity noncatalytic aryl phosphate binding site in which Arg-254 and Arg-24 are key residues. Compound **2** was found to bind to PTP1B in two mutually exclusive modes. In one mode, the one phosphate group binds in the catalytic site while the other phosphate makes a water-mediated hydrogen bond with Gln-262. In the other mode, one phosphate again makes a water-mediated hydrogen bond with Gln-262. However, the other phosphate group binds in the second aryl phosphate binding site. Each site was approximately 50% occupied. Two molecules of **2** are incapable of binding simultaneously to the enzyme as a result of steric repulsion between the two distal phosphate groups. On the basis of these studies, it was suggested that a compound that simultaneously occupies both aryl phosphate binding sites may be a potent inhibitor of PTP1B.[32] The possibility that some of the residues involved in the second noncatalytic site may be less conserved among PTPases than those found in the catalytic site suggests that such compounds could also be selective for PTP1B.[32]

Several years ago we reported that compounds such as **4** and **5**, bearing two DFMP groups, are in general more effective inhibitors than compounds bearing a single DFMP group.[23−25] The effect of the additional DFMP group on binding could be modest, such as with compound **5** (IC_{50} = 26 μM) versus compound **7** (IC_{50} = 95 μM), or it could be quite significant, such as with compound **4**, which exhibited a K_i of 1.5 μM with PTP1B and is a 2−3 orders of magnitude more effective inhibitor than compound **6**. Later, Taing et al. reported a wide range of non-peptidyl bis-DFMP compounds, several of which exhibited K_i's with PTP1B similar to that of compound **4**.[34] Very recently, Desmarais and co-workers reported that the tripeptide E−F_2Pmp−F_2Pmp is a potent inhibitor of PTP1B, exhibiting an IC_{50} of 40 nM, while the tripeptide F_2Pmp−E−F_2Pmp exhibits an IC_{50} of 400 nM.[35] This indicates that the high inhibitory potency of the E−F_2Pmp−F_2Pmp peptide is a result of its sequence and not its overall charge.

The presence of a second aryl phosphate binding site seems to have offered an explanation as to why compounds bearing two DFMP groups are more effective inhibitors than the analogous compounds bearing only a single DFMP group. Indeed, it has been suggested by Taing et al. and Desmarais et al. that the potencies of their bis-DFMP compounds were a result of the interaction of the two phosphonate groups with the two phosphate binding sites, although no structural evidence was given to support this supposition. In the case of the naphthyl inhibitor **5**, the distance separating the two DFMP groups is too short and the naphthyl ring too rigid to allow both DFMP groups to interact with both phosphate binding sites simultaneously, which suggests that the second DFMP group on **5** enhances inhibitory potency by interacting with residues that are not part of the second phosphate binding site. However, modeling studies suggested to us that the linker arm separating

the two DFMP groups in **4** was of sufficient length and flexibility to allow them to interact with the two phosphate binding sites simultaneously. Does the second DFMP group on inhibitor **4** occupy the second phosphate binding site? Why is compound **4** a better inhibitor than **5**? Is the second site an important motif for the development of potent and selective PTP1B inhibitors? In an attempt to answer these questions and to learn more about those features that are important for the rational design of small-molecule PTP1B inhibitors, we determined the X-ray crystal structures of PTP1B complexed with compounds **4** and **5**. In addition, the selectivity of compound **4**, as well as several other bis-DFMP-bearing inhibitors, for PTP1B versus seven other PTPs is also reported.

Results and Discussion

Crystallization and Crystal Packing. Extensive soaking experiments using various conditions including using various buffers, pH, inhibitor concentrations, and soaking time failed to produce crystals with the bound inhibitor, as evidently shown by the lack of difference in the electron density. This, however, is not surprising because previous experiments had shown that those ligands larger than inorganic phosphate could not be soaked in but rather they have to be cocrystallized.[32,36] Modification of the crystallization conditions of the native PTP1B led to the reproducible production square-plate cocrystals, the largest being ~0.15 mm × 0.15 mm × 0.05 mm in size. The only significant changes of crystallization conditions are pH (now 6.5 instead of 7.5) and the increased concentration of PEG 8000. The cocrystals were usually too small for diffraction experiments, although occasionally a diffraction-size crystal could be obtained by chance. The cocrystals also have external morphology different from that of the native PTP1B crystals. Although they both have the same space group and are very similar in *a* and *b* dimensions, there is an elongation (~2−5 Å) in the *c* axis in both complex crystals. Interestingly, *c* axis elongation has similarly occurred in another PTP1B complex involving a larger ligand such as phosphotyrosine peptide, where the *c* axis increased ~20 Å.[36] However, the elongation in the *c* axis does not simply create more space between molecules along the *c* axis to accommodate substrate or inhibitor; it changes the crystal packing completely, hence making solution of the structure by molecular replacement necessary.

Molecular replacement calculations gave a single sharp and unambiguous solution in both cases. For instance, in the case of the PTP1B−**4** complex, the correlation coefficient of the top peak is 64.6%, compared to the second peak of 37.6%. At the active site, a clear and unambiguous difference in electron density corresponding to the inhibitor was evident (Figure 1). In contrast, there was no observable difference density at the second binding site. The lack of the difference density remains unchanged after further refinement of the complex structure with the inclusion of the inhibitor and gradual inclusion of water molecules. The final models exhibit excellent geometry as examined using the program Procheck,[37] and the final refinement statistics are summarized in Table 1 for both complex structures.

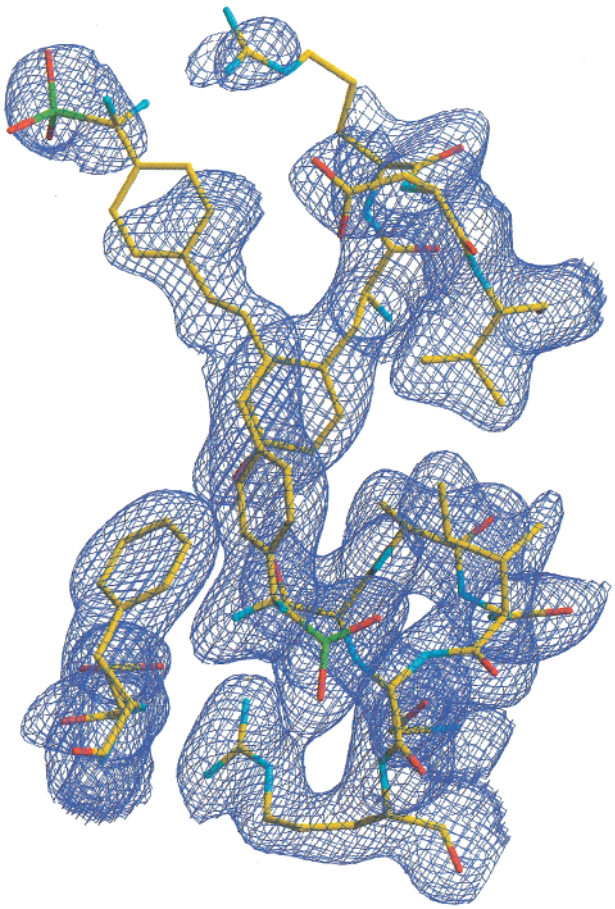

Figure 1. Electron density map of inhibitor **4** (contoured at σ), together with the final models of the inhibitor and PTP1B.

Table 1. Crystallographic Data and Refinement Statistics

	compound **4**	compound **5**
space group	$P3_121$	$P3_121$
a (Å)	89.22	87.52
b (Å)	89.22	87.52
c (Å)	108.78	106.29
resolution ranges (Å)	50.00−2.35	50.00−2.50
no. total reflns	89,257	61,055
no. unique reflns	20,176	13,400
R_{sym}	0.039	0.054
completeness (%)	92.2%	80.0%
refinement		
resolution ranges[a] (Å)	6.00−2.35	6.00−2.50
R (R_{free}, 10% random)	0.208 (0.250)	0.189 (0.254)
no. protein atoms	2,427	2,427
no. inhibitor atoms	30	24
no. water atoms	244	144
rmsd of bond length (Å)	0.011	0.008
rmsd of bond angles (deg)	1.41	1.47

[a] All data used with no σ cut.

Binding of Inhibitors to PTP1B. The complex structure of inhibitor **4** with PTP1B clearly shows that one of the DFMP groups (the proximal group) of the inhibitor occupies the active site (Figures 1−3). The binding mode is similar to those of all other complexes where the inhibitor/substrate has a similar aryl phosphate/phosphonate group.[22,38] As shown in Figure 4, the three terminal oxygen atoms accept hydrogen bonds from the main-chain amide groups of the PTP loop and form electrostatic interactions with Arg-221. There is a water molecule that is bound in a cavity that forms H bonds with the Pro-R fluorine, the N−H of Phe-182, and

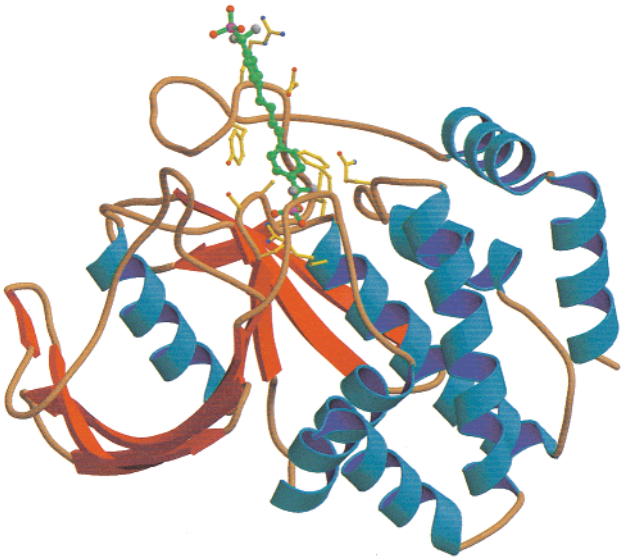

Figure 2. Ribbon diagram of PTP1B−**4** complex. Compound **4** is shown in ball and stick model. The extended conformation of compound **4** (shown in green) is evident. Side chains of contact residues of PTP1B are also shown.

one of the oxygens of the phosphonate group. The conformational change of the WPD loop takes place to close the active site. Phe-182, Tyr-46, and Val-49 may form hydrophobic interactions with the proximal phenyl ring and the proximal section of the hydrocarbon linker arm. Because of the exposed position of the protein region in the vicinity of the second aryl phosphate group, the number of contacts between the enzyme and **4** is limited and higher temperature factors of both the inhibitor and enzyme are observed, as evident by the weak and noncontinuous density in the solvent-exposed region (Figure 1). However, even though with the weak density, the extended conformation of the inhibitor, which only binds to the primary or active site, is beyond any doubt. Clearly, there is no difference density in the second site. Therefore, we conclude that this inhibitor does not bind to the second aryl phosphate-binding site. The hydrocarbon linker chain does not bend as is required to direct the distal phenyl DFMP group toward the second phosphate binding site. Instead, it extends into the solvent and is involved in water-mediated H-bonding interactions with Arg-47.

As fully expected, the proximal phosphate group of compound **5** binds to PTP1B similarly to the binding in PTP1B−**4** and other reported phosphonate complex structures.[22,38] Because of the shorter length of inhibitor **5**, it was not expected that it would be able to reach the second site. Indeed, the second phosphate group, extending straight from the aromatic moiety, makes little or no contact with the enzyme. Thus, the shorter inhibitor **5** is not able to make the critical water-mediated interaction between the second phosphate group and Arg-47 as observed in the inhibitor **4** complex, which is likely the main factor contributing to the different affinity between these two compounds. Interactions between Arg-47 and acidic residues in ligands and inhibitors have been noted by other workers. Arg-47 has been shown to provide key interactions with the Glu residue of the D-A-D-E-pY-L-NH_2 peptide.[36] Burke and co-workers have examined this interaction as a basis of rational inhibitor design.[39] These workers found that certain dipeptidyl and non-peptidyl difluoromethylphosphonic acids bearing carboxylic acid functionalities were better inhibitors of PTP1B than the parent compounds **6** and **7**. These results were consistent with molecular dynamics studies that suggested that some of this increase in affinity could be attributed to interactions between Arg-47 and the carboxyl group.

Bis-DFMP Inhibitors Bearing Alternative Linker Arms. Although our modeling studies suggested that a linker arm consisting of four CH_2 groups seems to be sufficient for allowing both DFMP groups to interact with the two phosphate binding sites, dual occupancy may require a longer linker that has more optimal

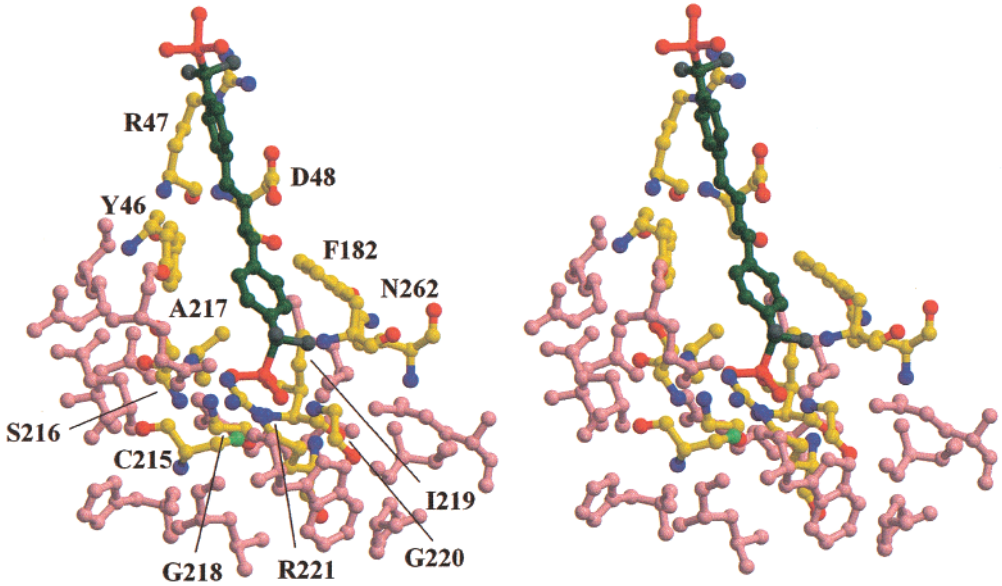

Figure 3. Stereodiagram of a closeup view of the PTP1B−**4** complex. The inhibitor and enzyme residues are represented in ball and stick model. The inhibitor is dark green. Residues that make immediate contact with the inhibitor are yellow, and those farther away are pink. Contact residues are also labeled.

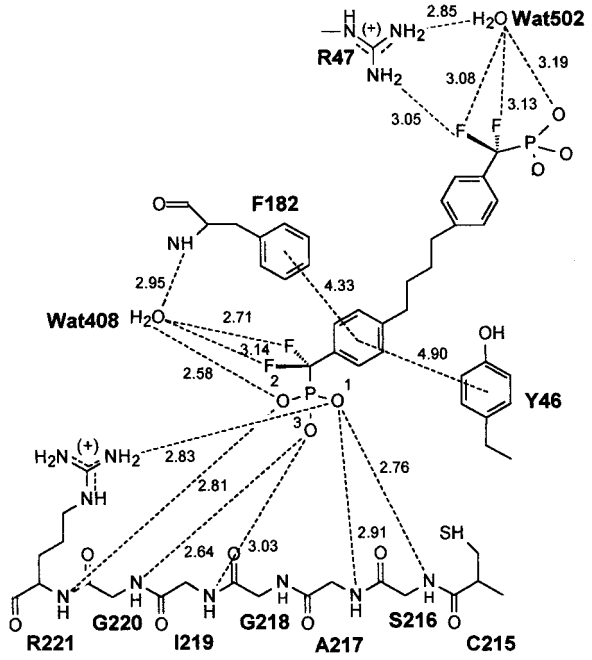

Figure 4. Schematic of inhibitor **4**−PTP1B interactions. A distance cutoff of 3.2 Å was used except for those involving certain aromatic rings.

length and, more importantly, afford more variation in torsion angle freedom. Because the two DFMP groups in **4** clearly do not interact with both binding sites, we prepared compound **8** (Scheme 1) in which the two aryl DFMP groups were joined by a longer yet still flexible linker, as well as compounds **9**−**11** (Scheme 2), in which the linker arm joining the two DFMP groups was longer yet was more rigid than the linker arms in inhibitors **4** and **8**. However, these compounds exhibited IC_{50} values (1.7−5.3 μM) with PTP1B that were similar to that obtained with compound **4** (Table 2). Thus, altering the length and flexibility of the linker arm made little difference in inhibitory potency. Analysis of the data obtained by Taing and co-workers on the inhibition of PTP1B with a wide variety of compounds bearing two DFMP groups[34] reveals a similar phenomenon.

Compounds **4** and **8**−**11** were examined for selectivity by comparing the IC_{50} values obtained for PTP1B with those obtained with seven other PTPases (Table 2). Compound **9** demonstrated poor selectivity for PTP1B versus all of the PTPases examined with the one exception being meg-1 for which it exhibited a 35-fold preference of PTP1B. With the exception of compound **9**, all of the compounds exhibited good selectivity for PTP1B when compared to Cdc25a and meg-1. For the other four compounds, selectivity for PTP1B versus PTPβ ranged from good (45- to 77-fold for compounds **4**, **8**, and **11**) to modest (15-fold for compound **10**). Similar trends in PTP1B selectivity with these four compounds were also found using CD45. The selectivity of all of the compounds for PTP1B versus TCPTP, SHP-1, and SHP-2 was modest to very poor. The only exception to this was compound **8**, which exhibited a 39-fold preference for PTP1B versus SHP-2. Compound **11** had previously been shown by Taing et al. to inhibit PTP1B with a K_i of 2.7 μM, which is similar to the IC_{50} value (1.7 μM) that we have obtained for **11** with PTP1B. Taing et al. also reported that compound **11** displayed little inhibitory potency with VHR or PTPα and was 18-fold less effective with LAR compared to PTP1B.[34] Our studies with compound **11** show that its selectivity is good compared to cdc25A and PTP-meg1, modest with SHP-2, CD45, and PTPβ, but very poor when compared to SHP-1 and TCPTP.

Inhibitor Potency and the Second Phosphate Binding Site. As mentioned earlier, Taing et al. recently reported PTP1B inhibition studies with a wide variety of compounds bearing two DFMP groups.[34] The best inhibitor from this series, compound **21**, exhibited

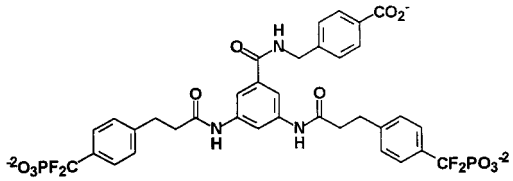

21

a K_i of 0.93 μM with PTP1B. Although it was suggested that the two DFMP groups in **21** interacted with the two phosphate binding sites in PTP1B, the possibility of less specific interactions with residues outside the second site was also raised. It is of significance that compound **4** (K_i = 1.5 μM), which exhibits an affinity for PTP1B that is only slightly less than compound **21**, interacts with Arg-47 and not the second phosphate binding site. It is also of significance that compounds **8**−**11** exhibit little difference in inhibitory potency with

Scheme 1

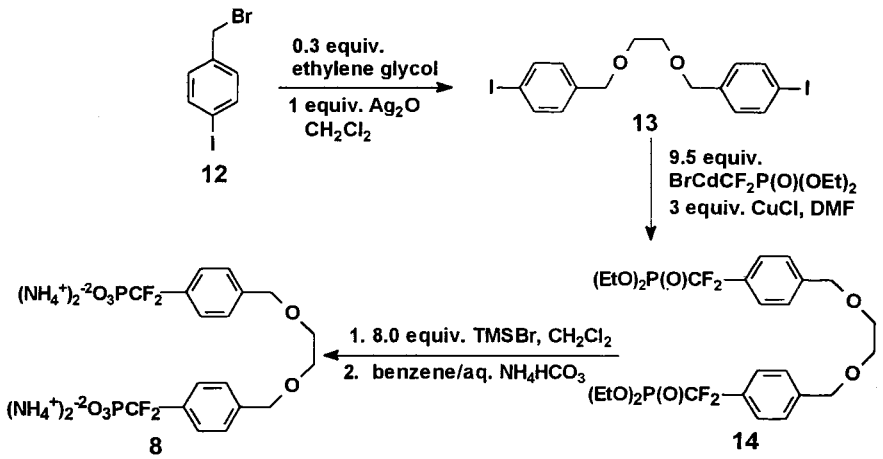

Scheme 2

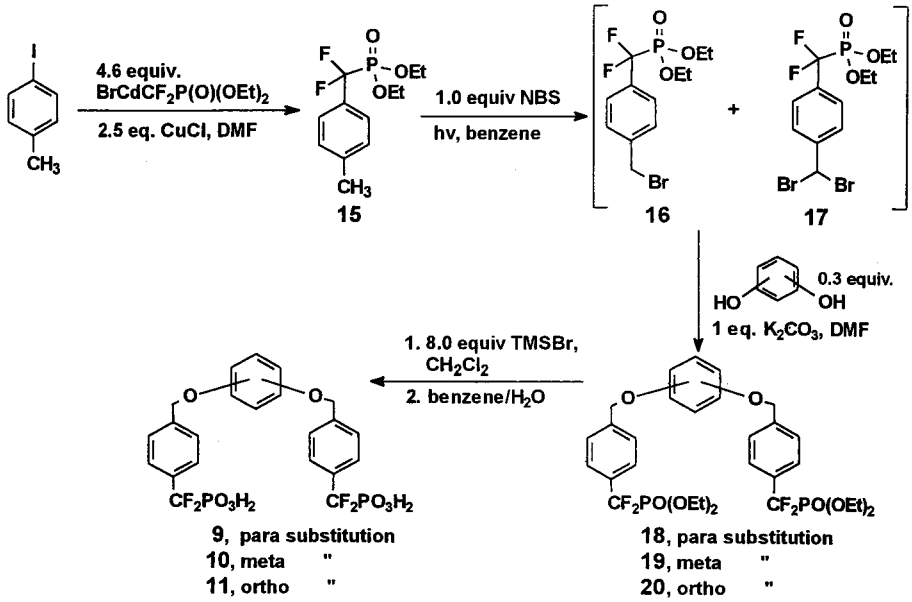

Table 2. IC_{50} Values of Inhibitors **4** and **8**−**11**

	IC_{50} (μM)							
compound	PTP1B	TCPTP	SHP-1	SHP-2	CD45	Cdc25a	PTPβ	PTPmeg-1
4	4.4	6.4	31	91	198	16% at 250 μM	342	9% at 250 μM
8	3.9	6.1	61	152	236	13% at 250 μM	300	2% at 250 μM
9	4.2	4.6	6.3	16	14	30	15	146
10	5.3	7.9	16	32	108	163	77	30% at 380 μM
11	1.7	3.2	15	60	42	163	77	30% at 500 μM

PTP1B compared to compound **4**, yet the length and flexibility of the units linking the two phenyl DFMP groups in compounds **8**−**11** differ significantly from that found in inhibitor **4**. Indeed, the potency of compounds **8**−**11** with PTP1B differs little from compound **21**, which has an even longer spacer separating the two phenyl DFMP groups. There are two possible explanations for these results. One possibility is that, despite the differences in the length and flexibility of the spacers separating the two phenyl DFMP groups in both our and Taing et al.'s studies, none of the compounds reported here or by Taing et al. interact with both phosphate binding sites simultaneously. The second phenyl DFMP increases inhibitory potency by interacting with other positive residues that are within the vicinity of the active site, of which there are several (Arg-43, Arg-45, Arg-47, Lys-36, Lys-116, Lys-120). The other possibility is that some of the compounds reported here and by Taing et al. do interact with the second site. However, if this is the case, then bis-DFMP inhibitors that interact with both phosphate binding sites may not be significantly more potent than bis-DFMP inhibitors that interact with both the catalytic site and other residues that are not part of the second site, such as Arg-47.

Although dual binding has yet to be established with PTP1B inhibitors, it has very recently been unequivocally demonstrated with pTyr-bearing substrates.[40] Salmeen et al. reported the crystal structure of C215A PTP1B complexed with the insulin receptor kinase (IRK) peptide, ETDpYpYRKGGKGGL, which bears two tandem pTyr residues.[40] This peptide exhibits a 70-fold greater affinity for a PTP1B substrate-trapping mutant (D181A-PTP1B) and a >10-fold lower K_m for PTP1B than the analogous peptide bearing a single pTyr residue (ETDYpYRKGGKGGL). Arg-47 forms a salt bridge with the Asp residue in the peptide. One of the pTyr residues binds in the catalytic site, while the other occupies the second phenylphosphate binding site. The phenyl ring of the substrate in the noncatalytic site is poorly ordered and may adopt a variety of conformations. This observation, along with mutagenesis studies, indicates that Arg-254 in the noncatalytic site is the main contributor to the enhanced affinity.[40] The distance between the two phosphate groups in the diphosphorylated IRK peptides reported by Salmeen et al. is greater than in compound **4**, which may explain why **4** does not exhibit dual binding. However, an array of nonpeptidyl compounds bearing two DFMP groups attached by linker arms of varying length and/or flexibility, reported here and by Taing et al.,[34] did not differ significantly from **4** in terms of inhibitory potency. We have shown that a significant increase in inhibitor potency, by over 2 orders of magnitude, can result from interaction of the second phosphate group by a water-mediated H bond with Arg-47. This is greater than the difference in affinity between the mono- and diphosphorylated IRK peptides.[40] This suggests that interaction of a phosphate group with Arg-254 may not be any more advantageous, in terms of inhibitor potency, than interaction with other positively charged residues in the vicinity of active site, such as Arg-47.

Selectivity and the Second Phosphate Binding Site. It is significant to note that all of the compounds reported in this study exhibited very poor selectivity for PTP1B versus TCPTP. TCPTP is abundantly and widely

expressed.[41] TCPTP is capable of dephosphorylating an 18-amino acid phosphopeptide bearing three phosphotyrosines that correspond to the autophosphorylated sequence of the insulin receptor kinase (IRK), and an Asp-Ala mutant of TCPTP was capable of trapping the entire intracellular IRK.[42] Unlike the PTP1B knock-out mice, TCPTP null mice die soon after birth.[43] This underscores the importance of obtaining inhibitors that are specific for PTP1B as far as their therapeutic potential is concerned. TCPTP and PTP1B exhibit a high degree of sequence homology.[44] Like PTP1B, TCPTP has an Arg at position 47 as well as all of the key residues in the second phosphate binding site such as Arg-24, Arg-254, Gly-259, and Met-258.[44] Thus, it is unlikely that Arg-47 or the second phosphate binding site will be useful motifs for obtaining inhibitors that are capable of differentiating between PTP1B and TCPTP. Nevertheless, it is possible that these motifs may be useful for obtaining inhibitors that are selective for PTP1B versus PTPs other than TCPTP. SHP-1 and SHP-2 have a Lys at the position corresponding to that of Arg-47 in PTP1B.[44,45] Several, but not all, of the key residues that constitute the second phosphate binding site, such as Arg-254, Gly-259, and Met-258, are present in SHP-1 and SHP-2.[44,45] These residues are less highly conserved in the receptor-like PTPs such as PTPβ and CD45.[44] The catalytic domain of cdc25a exhibits little structural homology to PTP1B.[46] Compound **21** reported by Taing et al. exhibited very good selectivity (100- to 3600-fold) for PTP1B versus the dual specificity PTPase VHR and the receptor-like PTPases LAR and PTPα. However, its selectivity with TCPTP was not reported. The tripeptide E$-F_2$Pmp$-F_2$Pmp, which is a potent inhibitor of PTP1B (K_i = 40 nM), was found to be at least 100-fold more selective for PTP1B versus CD45, LAR, PTPβ, and SHP-1.[35] Its selectivity with TCPTP was not reported.

Conclusions

Dual binding of PTP1B inhibitors has yet to be verified. Nevertheless, our results suggest that interaction of bis-DFMP-bearing inhibitors with Arg-47 can result in a significant increase in inhibitor potency and that interaction with this residue may be just as effective a means of increasing inhibitor potency as interaction with the second phosphate binding site. Our results from selectivity experiments clearly demonstrate a further challenge in developing highly specific inhibitors toward PTP1B as reflected by the virtual nonexistence of selectivity toward PTP1B and TCPTP. Given the extremely high sequence identity between these two enzymes, it is not surprising that poor selectivity was observed. It is unlikely that inhibitors that target either the second phosphate binding site or Arg47 will be selective for PTP1B vs TCPTP. Finally, the limited membrane permeability of DFMP-bearing compounds[22] must also be addressed. The use of less highly charged phosphate mimetics is currently being examined as a means of avoiding this problem.[47,48]

Experimental Section

General. All starting materials for syntheses were obtained from commercial suppliers (Aldrich Chemical Co., Oakville, Ontario, Canada, or Lancaster Synthesis Incorporated, Windham, NH). Trimethylsilyl bromide (TMSBr) was freshly distilled before use. Solvents were purchased from Caledon Laboratories (Georgetown, Ontario, Canada), Lancaster Synthesis Incorporated, and BDH Canada (Toronto, Canada). Tetrahydrofuran (THF) was distilled from sodium metal in the presence of benzophenone under argon. CH_2Cl_2 was distilled from calcium hydride under argon. Dimethylformamide (DMF) was distilled under reduced pressure from calcium hydride and stored over 4 Å sieves under argon. Reactions involving moisture-sensitive reagents were executed under an inert atmosphere of dry argon or nitrogen. All glassware was predried prior to use, and all liquid transfers were performed using dry syringes and needles. Silica gel chromatography was performed using silica gel 60A (Silicycle, 230−400 mesh). ^{1}H, ^{19}F, ^{31}P, and ^{13}C NMR spectra were recorded on a Varian 200-Gemini, Bruker AC-200, and Bruker AC-300 NMR spectrometers. The abbreviations s, d, t, q, m, dd, dt, and br are used for singlet, doublet, triplet, quartet, multiplet, doublet of doublets, doublet of triplets, and broad, respectively. Chemicals shifts (δ) for ^{1}H NMR spectra run in $CDCl_3$ are reported in ppm relative to the internal standard tetramethylsilane (TMS). Chemical shifts (δ) for ^{1}H NMR spectra run in CD_3OD are reported in ppm relative to residual solvent protons (δ 3.30). Chemical shifts (δ) for ^{1}H NMR spectra run in D_2O are reported in ppm relative to residual solvent protons (δ 4.79). For ^{13}C NMR spectra run in $CDCl_3$, chemical shifts are reported in ppm relative to the $CDCl_3$ residual carbons (δ 77.0 for central peak). For ^{13}C NMR spectra run in CD_3OD, chemical shifts are reported in ppm relative to the CD_3OD residual carbons (δ 49.0 for central peak). For ^{13}C NMR spectra run in D_2O, chemical shifts are reported in ppm relative to CH_3OH in D_2O (external). For ^{31}P NMR spectra, chemical shifts are reported in ppm relative to 85% phosphoric acid (external). For ^{19}F NMR spectra, chemical shifts are reported in ppm relative to trifluoroacetic acid (external). Low-resolution and high-resolution electron impact mass spectra (EIMS) were obtained on a Micromass 70-S-250 mass spectrometer. Low-resolution electrospray ionization mass spectra (LRES-IMS) were obtained on a Micromass Quatro II mass spectrometer. High-resolution electrospray ionization mass spectra (HRESMS) were obtained on a Micromass ZabSpec oaTOF spectrometer. All melting points were taken on a Mel-Temp melting point apparatus and are uncorrected. Analytical HPLC was performed on a Waters 600E LC system using a Vydac 218TP54 analytical C-18 reverse-phase column and a Waters 2487 absorbance detector set at 254 nm. Enzyme assay solutions were prepared with deionized/distilled water. Compounds **4** and **5** were prepared as previously described.[49,50] T-cell PTP was obtained from Calbiochem (human, recombinant *E. coli*, catalog no. 539732, lot no. B21267).

1-Iodo-4-(2benzyloxyethoxymethyl)benzene (13). To a solution of *p*-iodobenzyl bromide (**12**, 2.1 g, 7.07 mmol, 3 equiv) in anhydrous CH_2Cl_2 (5 mL) was added ethylene glycol (0.13 mL, 2.33 mmol, 1 equiv) and silver(I) oxide (1.64 g, 7.08 mmol, 3 equiv). The reaction mixture was stirred for 48 h at room temperature and filtered, and the filtrate was concentrated by rotary evaporation. Pure **13** was obtained as a white solid (0.60 g, 52%) after purification via flash chromatography (EtOAc/hexane, 20:80, R_f = 0.3) and recrystallization in CH_2Cl_2/hexane: mp 75−77 °C; ^{1}H NMR (200 MHz, $CDCl_3$) δ 7.67 (d, J = 8.7 Hz, 4H, aryl), 7.09 (d, J = 7.3 Hz, 4H, aryl), 4.51 (s, 4H, 2(CH_2Ar)), 3.64 (s, 4H, OCH_2CH_2O); ^{13}C NMR (50 MHz, $CDCl_3$) δ 138.2, 137.5, 129.5, 92.9, 72.7, 69.9; LREIMS *m*/*z* 494 (M^+, trace), 277 (loss of CH_2ArI, 100%); HRMS(EI) calcd for $C_{16}H_{16}O_2I_2$ 493.9239, found 493.9229.

{**[4-(2-{4-[(Diethoxyphosphoryl)difluoromethyl]benzyloxy}ethoxymethyl)phenyl]difluoromethyl}phosphonic Acid Diethyl Ester (14).** Diethylbromodifluoromethane phosphonate (2.7 mL, 15.2 mmol, 9.5 equiv) was added to a stirring suspension of cadmium powder (1.8 g, 16.0 mmol, 10 equiv) in anhydrous DMF (10 mL), and the mixture was stirred for 4 h in a round-bottom flask fitted with a condenser (exothermic reaction). The mixture was then filtered quickly under an inert atmosphere through oven-dried Celite into a round-bottom flask containing **13** (0.8 g, 1.6 mmol, 1.0 equiv) and copper(I)

chloride (0.8 g, 8.1 mmol, 5.1 equiv), and the mixture was stirred for 12 h. The mixture was filtered, and the filtrate was transferred to a separatory funnel, to which was added CH_2Cl_2 (30 mL). The organic layer was washed with water (2 × 25 mL), 5% $NaHCO_3$ (1 × 25 mL), and brine (1 × 25 mL), dried ($MgSO_4$), filtered, and concentrated by rotary evaporation. **14** was purified via silica gel chromatography (EtOAc/hexane, 55:45, $R_f = 0.4$) and was obtained in pure form as a colorless oil (0.78 g, 79%). ^{1}H NMR (200 MHz, $CDCl_3$) δ 7.59 (d, $J = 8.0$ Hz, 4H, aryl), 7.43 (d, $J = 8.1$ Hz, 4H, aryl), 4.62 (s, 4H, 2(CH_2-Ar)), 4.17 (m, 8H, 4(OCH_2CH_3)), 3.69 (s, 4H, OCH_2CH_2O)), 1.30 (t, $J = 7.0$ Hz, 12H, 4(OCH_2CH_3)); ^{13}C NMR (50 MHz, $CDCl_3$) δ 141.4, 132.0, 127.3, 126.4, 118.1 (td, $J_{CF} = 263.5$ Hz, $J_{CP} = 217.8$ Hz), 72.7, 70.0, 64.6 (d, $J_{CP} = 6.4$ Hz), 16.2 (d, $J_{CP} = 5.5$ Hz); ^{19}F NMR (188 MHz, $CDCl_3$) δ −32.25 (d, $J_{FP} = 117.5$ Hz); ^{31}P NMR (81 MHz, $CDCl_3$) δ 4.13 (t, $J_{PF} = 117.5$ Hz); LREIMS *m/z* 616 ($M^+ + H^+$, trace), 278 ($CH_2ArCF_2P(O)(OEt)_2 + H^+$, 77%), 140 (100%).

{[4-(2-{4-[(Diethoxyphosphoryl)difluoromethyl]benzyloxy}ethoxymethyl)phenyl]difluoromethyl}phosphonic Acid (8). To a solution of ester **14** (0.100 g, 0.16 mmol, 1 equiv) in dry CH_2Cl_2 (4 mL) was added TMSBr (0.17 mL, 1.3 mmol, 8 equiv), and the solution was refluxed for 2 days under an argon atmosphere. The solvent was removed by rotary evaporation, the resulting oil was dissolved in dry CH_2Cl_2, and the solution was concentrated again by rotary evaporation. This process was repeated two more times. The resulting colorless oil was then placed under high vacuum for 16 h to remove any traces of unreacted TMSBr. The oil was redissolved in benzene (3 mL), and an aqueous solution (3 mL) of NH_4HCO_3 (0.077 g, 0.97 mmol, 6 equiv) was added. After the mixture was vigorously stirred for 30 min, the organic layer was evaporated and the aqueous solution was lyophilized repeatedly to yield **8** as a pure, white solid in near-quantitative yield (0.093 g). ^{1}H NMR (200 MHz, D_2O) δ 7.63 (d, $J = 7.7$ Hz, 4H, aryl), 7.49 (d, $J = 8.0$ Hz, 4H, aryl), 4.65 (s, 4H, 2(CH_2Ar)), 3.74 (s, 4H, OCH_2CH_2O); ^{13}C NMR (50 MHz, D_2O) δ 139.8, 133.7 (m), 127.9, 126.0 (t, $J = 6.6$ Hz), 119.8 (weak td), 72.0, 68.9; ^{19}F NMR (188 MHz, D_2O) δ −28.36 (d, $J_{FP} = 96.1$ Hz); ^{31}P NMR (202.5 MHz, D_2O) δ 4.65 (t, $J_{PF} = 96.4$ Hz); LRESIMS *m/z* 501.1 (monoanion, loss of 4 × NH_4^+, gain of $3H^+$), 250.1 (dianion, loss of 4 × NH_4^+, gain of $2H^+$); HRESMS calcd for $C_{18}H_{19}F_4O_8P_2$ 501.0485, found 501.0485. Analytical HPLC analysis of the ammonium salt was performed using acetonitrile (solvent A) and 0.1% TFA in water (solvent B) as eluants under the following conditions: linear gradient of 5% A/95% B to 100% A (5 min), 100% A (10 min), linear gradient of 100% A to 5% A/95% B (5 min), 100% B (10 min). Only a single peak was evident on the HPLC chromatogram. Retention time was 7.6 min.

(Difluoro-*p*-tolylmethyl)phosphonic Acid Diethyl Ester (15). Diethylbromodifluoromethane phosphonate (14.5 mL, 82.0 mmol, 4.6 equiv) was added to a stirring suspension of cadmium (10.0 g, 89.0 mmol, 5.0 equiv) in anhydrous DMF (50 mL), and the mixture was stirred for 4 h in a round-bottom flask fitted with a condenser (exothermic reaction). The mixture was then filtered quickly under an inert atmosphere through oven-dried Celite into a round-bottom flask containing *p*-iodotoluene (3.90 g, 18.0 mmol, 1.0 equiv) and copper(I) chloride (4.39 g, 44.0 mmol, 2.5 equiv), and the mixture was stirred for 12 h at room temperature. The mixture was filtered, and the filtrate was transferred to a separatory funnel, to which was added CH_2Cl_2 (100 mL). The solution was washed with water (2 × 50 mL), 5% $NaHCO_3$ (1 × 50 mL), and brine (1 × 50 mL), dried ($MgSO_4$), filtered, and concentrated by rotary evaporation. Pure **15** was obtained by silica gel chromatography (EtOAc/hexane, 30:70, $R_f = 0.5$) as a colorless oil (4.05 g, 82%). ^{1}H NMR (200 MHz, $CDCl_3$) δ 7.51 (d, $J = 7.3$ Hz, 2H, aryl), 7.25 (d, $J = 8.8$ Hz, 2H, aryl), 4.20 (m, 4H, 2(OCH_2CH_3)), 2.40 (s, 3H, CH_3), 1.31 (t, $J = 7.3$ Hz, 6H, 2(OCH_2CH_3)); ^{13}C NMR (50 MHz, $CDCl_3$) δ 140.9, 129.6 (m), 129.0, 126.1 (br t), 118.2 (weak td, CF_2), 64.5 (d, $J_{CP} = 6.4$ Hz), 21.1, 16.1 (d, $J_{CP} = 3.7$ Hz); ^{19}F NMR (188 MHz, $CDCl_3$) δ −32.09 (d, $J_{FP} = 119.0$ Hz); ^{31}P NMR (81 MHz, $CDCl_3$) δ 4.35 (t, $J_{PF} = 117.5$ Hz); LREIMS *m/z* 278 (M^+, 16%), 141 ($M^+ - P(O)(OEt)_2$, 100%); HRMS(EI) calcd for $C_{12}H_{17}O_3F_2P$ 278.0883, found 278.0889.

Synthesis of 18−20. General Procedure. A solution of **15** (1.0 equiv) and *N*-bromosuccinimide (1.1 equiv) in benzene (60 mL per gram of **15**) was irradiated using a reflector IR heat lamp (250 W, 120 v) for 1.5 h. The solution was washed with water, 5% $NaHCO_3$, and brine, dried ($MgSO_4$), and concentrated by rotary evaporation. The desired product was partially purified by silica gel chromatography (EtOAc/toluene, 30:70, $R_f = 0.4$) to yield a clear, colorless oil. ^{1}H NMR analysis of the crude material indicated a mixture of the desired product **16**, the undesired dibrominated material **17**, and unreacted **15** in a 68:6.5:25.5 ratio. This mixture was used without any further purification for the synthesis of **18**−**20**. To a solution of the diol (hydroquinone, resorcinol, or catechol, 0.3 equiv) and K_2CO_3 (1.0 equiv) in anhydrous DMF (12 mL/mmol diol) was added a solution of crude **16** (approximately 1.0 equiv of **16**) and anhydrous DMF (5 mL of DMF/g of crude material). After 12 h, EtOAc (90 mL/mmol of diol) was added and the organic layer was washed twice with water and once with brine (90 mL/mmol of diol of each aqueous solution). The organic layer was dried ($MgSO_4$), filtered, and concentrated by rotary evaporation. Pure **18**−**20** was obtained by silica gel chromatography as a white crystalline solid or as a colorless oil. Yields are based on the diol as the limiting reagent.

[(4-{4-[4-(Difluorophosphonomethyl)benzyloxy]phenoxymethyl}phenyl)difluoromethyl]phosphonic acid diethyl ester (18): white solid; yield, 44%; mp 91−93 °C; TLC $R_f = 0.3$ (EtOAc/CH_2Cl_2, 12:88); ^{1}H NMR (200 MHz, $CDCl_3$) δ 7.64 (d, $J = 7.6$ Hz, 4H, aryl), 7.51 (d, $J = 8.4$ Hz, 4H, aryl), 6.90 (s, 4H, aryl), 5.07 (s, 4H, 2(CH_2Ar)), 4.20 (m, 8H, 4(OCH_2CH_3)), 1.32 (t, $J = 7.0$ Hz, 12H, 4(OCH_2CH_3)); ^{13}C NMR (50 MHz, $CDCl_3$) δ 153.3, 140.3, 132.3 (m) 127.1, 126.5, 118.0 (weak td), 116.1, 70.3, 64.7 (d, $J_{CP} = 6.4$ Hz), 16.3 (d, $J_{CP} = 4.6$ Hz); ^{19}F NMR (188 MHz, $CDCl_3$) δ −32.30 (d, $J_{FP} = 116.0$ Hz); ^{31}P NMR (81 MHz, $CDCl_3$) δ 4.07 (t, $J_{PF} = 116.0$ Hz); LREIMS *m/z* 662 (M^+, 40%), 277 ($CH_2ArCF_2P(O)(OEt)_2$, 100%); HREIMS calcd for $C_{30}H_{36}O_8F_4P_2$ 662.1822, found 662.1788.

[(4-{3-[4-(Difluorophosphonomethyl)benzyloxy]phenoxymethyl}phenyl)difluoromethyl]phosphonic acid diethyl ester (19): colorless oil; yield, 76%; TLC $R_f = 0.5$ (EtOAc/hexane, 70:30); ^{1}H NMR (200 MHz, $CDCl_3$) δ 7.64 (d, $J = 7.3$ Hz, 4H, aryl), 7.51 (d, $J = 7.3$ Hz, 4H, aryl), 7.18 (t, $J = 8.8$ Hz, 1H, aryl), 6.58 (m, 3H, aryl), 5.08 (s, 4H, 2(CH_2Ar)), 4.20 (m, 8H, 4(OCH_2CH_3)), 1.30 (t, $J = 7.3$ Hz, 12H, 4(OCH_2CH_3)); ^{13}C NMR (50 MHz, $CDCl_3$) δ 160.0, 140.1, 133.1 (m), 130.0, 127.1, 126.6 (br t), 118.1 (td, $J_{CF} = 263.5$ Hz, $J_{CP} = 218.0$ Hz), 107.9, 102.8, 69.6, 64.6 (d, $J_{CP} = 6.4$ Hz), 16.2 (d, $J_{CP} = 5.5$ Hz); ^{19}F NMR (188 MHz, $CDCl_3$) δ −32.30 (d, $J_{FP} = 116.7$ Hz); ^{31}P NMR (81 MHz, $CDCl_3$) δ 4.13 (t, $J_{PF} = 117.5$ Hz); LREIMS *m/z* 662 (M^+, trace), 642 (loss of HF, 100%), 277 ($CH_2ArCF_2P(O)(OEt)_2$, 50%); HREIMS calcd for $C_{30}H_{36}O_8F_4P_2$ 662.1822, found 662.1806.

[(4-{2-[4-(Difluorophosphonomethyl)benzyloxy]phenoxymethyl}phenyl)difluoromethyl]phosphonic acid diethyl ester (20): colorless oil; yield, 69%; TLC $R_f = 0.3$ (EtOAc/CH_2Cl_2, 12:88); ^{1}H NMR (200 MHz, $CDCl_3$) δ 7.59 (m, 8H, aryl), 6.90 (m, 4H, aryl), 5.21 (s, 4H, 2(CH_2Ar)), 4.18 (m, 8H, 4(OCH_2CH_3)), 1.31 (t, $J = 7.1$ Hz, 12H, 4(OCH_2CH_3)); ^{13}C NMR (50 MHz, $CDCl_3$) δ 149.1, 140.4, 132.4 (m), 127.1, 126.5 (t, $J = 6.0$ Hz), 122.1, 118.0 (weak td), 115.9, 71.0, 64.6 (d, $J_{CP} = 6.4$ Hz), 16.2 (d, $J_{CP} = 4.6$ Hz); ^{19}F NMR (188 MHz, $CDCl_3$) δ −32.31 (d, $J_{FP} = 116.0$ Hz); ^{31}P NMR (81 MHz, $CDCl_3$) δ 4.05 (t, $J_{PF} = 116.0$ Hz); LREIMS *m/z* 662 (M^+, 7%), 642 (loss of HF, 50%), 277 ($CH_2ArCF_2P(O)(OEt)_2$, 100%); HREIMS calcd for $C_{30}H_{36}O_8F_4P_2$ 662.1822, found 662.1799.

Synthesis of 9−11. General Procedure. To a solution of the ethyl ester **18**, **19**, or **20** (1.0 equiv) in dry CH_2Cl_2 (9 mL/0.1 mmol ester) was added TMSBr (8 equiv), and the solution was refluxed for 2 days under an argon atmosphere. The solvent was removed by rotary evaporation, the resulting oil was dissolved in dry methylene chloride, and the solution was concentrated again by rotary evaporation. This process was

repeated two more times. The resulting colorless oil was then placed under high vacuum for 16 h. The oil was redissolved in benzene (3 mL), and water (3 mL) was added. After the mixture was vigorously stirred for 30 min, the organic layer was removed by rotary evaporation and the aqueous solution was lyophilized to yield pure **9**−**11** as white solids in near-quantitative yield. The acids were converted to their ammonium salts by addition of an aqueous solution of 2.5 equiv of ammonium bicarbonate followed by repeated lyophilization until a constant weight was obtained. The compounds were analyzed by analytical HPLC as described above for compound **8**. All compounds showed only a single peak in the HPLC chromatogram.

[(4-{4-[4-(Difluorophosphonomethyl)benzyloxy]phenoxymethyl}phenyl)difluoromethyl]phosphonic acid (9): ^{1}H NMR (200 MHz, CD_3OD) δ 7.63 (d, J = 8.0 Hz, 4H, aryl), 7.53 (d, J = 8.0 Hz, 4H, aryl), 6.93 (s, 4H, aryl), 5.10 (s, 4H, CH_2Ar); ^{13}C NMR (125 MHz, CD_3OD) δ 154.4, 141.5, 134.7 (m), 128.1, 127.5 (t, J = 6.8 Hz), 116.9, 70.9; ^{19}F NMR (188 MHz, D_2O) δ −29.82 (d, J_{FP} = 105.2 Hz); ^{31}P NMR (81 MHz, D_2O) δ 4.47 (t, J_{PF} = 105.2 Hz); LRESMS *m*/*z* 549 (monoanion, loss of 1H$^+$), 274 (dianion, loss of 2H$^+$); HRESMS calcd for $C_{22}H_{19}F_4O_8P_2$ 549.0485, found 549.0480. HPLC retention time was 8.14 min.

[(4-{3-[4-(Difluorophosphonomethyl)benzyloxy]phenoxymethyl}-henyl)difluoromethyl]phosphonic acid (10): ^{1}H NMR (200 MHz, D_2O) δ 7.52 (d, J = 7.3 Hz, 4H, aryl), 7.37 (d, J = 8.8 Hz, 4H, aryl), 7.06 (t, J = 8.0 Hz, 1H, aryl), 6.50 (m, 3H, aryl), 4.92 (s, 4H, 2(CH_2Ar)); ^{13}C NMR (75 MHz, D_2O) δ 159.2, 137.9, 136.1 (m), 130.7, 127.8, 126.5 (t, J = 6.8 Hz), 108.6, 102.8, 70.1; ^{19}F NMR (188 MHz, D_2O) δ −30.00 (d, J_{FP} = 105.3 Hz); ^{31}P NMR (81 MHz, D_2O) δ 4.56 (t, J_{PF} = 106.0 Hz); LRESMS *m*/*z* 549 (monoanion, loss of 1H$^+$), 274 (dianion, loss of 2H$^+$); HRESMS calcd for $C_{22}H_{19}F_4O_8P_2$ 549.0485, found 549.0491. HPLC retention time = 8.02 min.

[(4-{2-[4-(Difluorophosphonomethyl)benzyloxy]phenoxymethyl}phenyl)difluoromethyl]phosphonic Acid (11): ^{1}H NMR (200 MHz, D_2O) δ 7.47 (d, J = 8.8 Hz, 4H, aryl), 7.29 (d, J = 7.4 Hz, 4H, aryl), 6.70 (bdt, 4H, aryl), 4.87 (s, 4H, 2(CH_2-Ar)); ^{13}C NMR (75 MHz, D_2O) δ 147.7, 139.0, 134.0 (m), 127.7, 126.2 (t, J = 6.8 Hz), 122.3, 119.9 (td, J_{CF} = 261.0 Hz, J_{CP} = 201.0 Hz), 115.4, 70.6; ^{19}F NMR (188 MHz, D_2O) δ −29.98 (d, J_{FP} = 106.9 Hz); ^{31}P NMR (81 MHz, D_2O) δ 4.64 (t, J_{PF} = 106.1 Hz); LRESMS *m*/*z* 549 (monoanion, loss of 1H$^+$), 274 (dianion, loss of 2H$^+$); HRESMS calcd for $C_{22}H_{19}F_4O_8P_2$ 549.0485, found 549.0485. HPLC retention time was 7.91 min.

Purification of PTPases. The flag-PTP1B (1−320) and flag-CD45 (intracellular domain) were purified as described by Huyer et al.[51] and Wang et al.[52] The GST-PTPβ, GST-SHP1, and GST-SHP2 were purified as previously reported.[35] CDC25a cDNA was obtained from osteoblast total RNA using the GeneAmp RNA PCR kit (Perkin-Elmer Cetus, CT). BamH1 and EcoR1 were added at the 5′ and 3′ end, respectively, during amplification. The recombinant baculovirus was prepared using the Bac-to-Bac baculovirus expression system (Gibco BRL, MD). The CDC25a DNA fragment was ligated in a pFastBac1 plasmid that was engineered to include a FLAG sequence at the 5′ end of the cDNA. Recombinant bacmid was obtained by transformation into competent cells DH10BAC *Escherichia coli* cells. The resultant was transfected into *Spodoptera frugiperda* Sf9 cells, and the virus found in the supernatant medium was amplified two times up to total viral stock volume of 500 mL. Production of the recombinant CDC25a was done essentially as described by Summers and Smith.[53] Sf9 cells were infected in Graces supplemented medium (TNM-FH) at a density of (1−3) × 10^6 cells/mL with the appropriate amount of viral stock (moi 5). The cells were cultured in suspension at 27 °C and were harvested at 72 h postinfection. The cell pellet was washed twice in ice-cold PBS and frozen at −80 °C until purification. All subsequent steps were carried out at 4 °C. The cell pellet (40 g) was lysed in 40 mL of lysis buffer (40 mM Tris-HCl, pH 7.5, 0.2% Triton X-100, 4 mM DTT, 4 mM EDTA, and one complete protease inhibitor tablet) and sonicated four times for 30 s on ice. The lysate was centrifuged at 10 000*g* in a SS34 rotor for 15 min. The supernatant was then centrifuged at 43 000*g* in a 50.2 Ti rotor in a Beckman ultracentrifuge for 50 min. The supernatant was applied to a 12 mL M2 flag (Sigma) monoclonal affinity column that was prepared as follows. The resin was washed with three column volumes of low-salt buffer (20mM Tris-HCl, pH 8, 150 mM NaCl, 1 mM DTT, and 2% Tween-20), then was activated with two column volumes of 0.1 M glycine pH 3, and finally was washed with three column volumes of low-salt buffer. The flow through was collected, and Tween-20 was added to a final concentration of 1% (v/v). This was reapplied to the same anti-flag affinity resin, and the mixture was washed with 10 column volumes of high-salt buffer (20 mM Tris-HCl, pH 8, 500 mM NaCl, 1 mM DTT, and 2% Tween-20) followed by 5 column volumes of low-salt buffer. The flag−CDC25a was eluted with 4 column volumes of low-salt buffer containing 0.17 mg/mL flag peptide. DTT to a final concentration of 5 mM was added to each fraction. Approximately 12 mg of flag−CDC25a (>80% pure as estimated by SDS−PAGE) were obtained.

Inhibition Studies. PTPase assays were performed using 3,6-fluorescein diphosphate (FDP) as substrate as previously described.[35] IC_{50} values were obtained using 10 different concentrations of inhibitor and at FDP concentrations approximately equal to the K_M concentration for each enzyme. Data were fit to the four-parameter equation[16] with errors less than 10% for all IC_{50} values obtained.

Crystallization of PTP1B−4 and PTP1B−5 Complexes. All crystallization experiments were carried out at 4 °C using the hanging-drop vapor diffusion method. Native PTP1B crystals were grown according to the published conditions[54] with one modification, namely, using 18−20% instead of 12−16% PEG 8000. In soaking experiments, PTP1B native crystals were placed in the inhibitor solution over a range of concentrations (from 5 to 20 mM) and time periods (from 2 to 36 h). For cocrystallization, the protein stock solution consists of 10 mg/mL PTP1B in a mixture of 10 mM Tris-HCl, 25 mM NaCl, 0.2 mM EDTA, 3.0 mM DTT, and 0.1 mM inhibitor **4** or **5**. For the PTP1B−**4** complex, a 2 μL drop of this stock solution was mixed with an equal volume of precipitating solution consisting of 19% PEG 8000, 0.1 M Hepes (pH 7.5), and 0.2 M magnesium acetate and was equilibrated against 1 mL of the precipitating solution. The conditions for PTP1B−**5** are identical except the buffer pH was changed to 6.7.

Diffraction Data Collection. Diffraction data were collected at the F1 station of Cornell High Energy Synchrotron Source (CHESS). For cryoprotection, crystals were serially transferred to crystallization solutions supplemented with 5%, 10%, 20%, and 25% glycerol for 2 min at each concentration followed by immediate flash cooling in liquid propane. Data collection was carried out in a stream of nitrogen gas at 100 K. The PTP1B−**4** and PTP1B−**5** crystals diffracted to 2.35 and 2.50 Å, respectively. Data were processed using Denzo/Scalepack,[55] and the data statistics are summarized in Table 1.

Structure Determination and Refinement. Molecular replacement calculations were carried out using the program EPMR,[56] with the probing model being the native PTP1B peptide complex structure devoid of the peptide.[36] After the first round of refinement using CNS,[57] clear and unambiguous difference electron density was evident in the active-site pocket in both PTP1B−**4** and PTP1B−**5**. A model of the inhibitor was then built and fitted in the difference density. The structure was refined, and water molecules were gradually added. Diagrams were prepared using Xtalview,[58] Molscript,[59] and Raster3D.[60] Coordinates of PTP1B−**4** and PTP1B−**5** complex structures have been deposited in the Protein Data Bank (accession codes: 1KAK and 1KAV).

Acknowledgment. This work was supported in part by the Natural Sciences and Engineering Research Council of Canada (NSERC) in the form of operating grants to Z.J. and S.D.T. and a postgraduate scholarship to A.N.D. Z.J. holds a Canada Research Chair in Structural Biology. The assistance from CHESS staff during

data collection is greatly appreciated. Brent Wathen helped with the diagrams.

References

(1) Neel, B. G.; Tonks, N. K. Protein tyrosine phosphatases in signal transduction. *Curr. Opin. Cell Biol.* **1997**, *9*, 193−204.

(2) Denu, J. M.; Stuckey, J. A.; Saper, M. A.; Dixon, J. E. Form and function in protein dephosphorylation. *Cell* **1996**, *87*, 361−364.

(3) Li, L.; Dixon, J. E. Form, function, and regulation of protein tyrosine phosphatases and their involvement in human diseases. *Semin. Immunol.* **2000**, *12*, 75−84.

(4) Jia, Z. Protein phosphatases: structures and implications. *Biochem. Cell Biol.* **1997**, *75*, 17−26.

(5) Zhang, Z. Y. Protein-tyrosine phosphatases: biological function, structural characteristics, and mechanism of catalysis. *Crit. Rev. Biochem. Mol. Biol.* **1998**, *33*, 1−5.

(6) Kennedy, B. P.; Ramachandran, C. Protein tyrosine phosphatase-1B in diabetes. *Biochem. Pharmacol.* **2000**, *60*, 877−883.

(7) Elchebly, M.; Payette, P.; Michaliszyn, E.; Cromlish, W.; Collins, S.; Loy, A. L.; Normandin, D.; Cheng, A.; Himms-Hagen, J.; Chan, C. C.; Ramachandran, C.; Gresser, M. J.; Tremblay, M. L.; Kennedy, B P. Increased insulin sensitivity and obesity resistance in mice lacking the protein tyrosine phosphatase-1B gene. *Science* **1999**, *283*, 1544−1548.

(8) Weiner, J. R.; Kerns, B. J.; Harvey, E. L.; Conaway, M. R.; Iglehart, J. D.; Berchuck, A.; Bast, R. C. Overexpression of the protein tyrosine phosphatase PTP1B in human breast cancer: association with p185c-erbB-2 protein expression. *J. Natl. Cancer Inst.* **1994**, *86*, 372−378.

(9) Liu, F.; Hill, D. E.; Chernoff, J. Direct binding of the proline-rich region of protein tyrosine phosphatase 1B to the Src homology 3 domain of p130(Cas). *J. Biol. Chem.* **1996**, *271*, 31290−31295.

(10) Burke, T. R., Jr.; Zhang, Z.-Y. Protein-tyrosine phosphatases: structure, mechanism, and inhibitor discovery. *Biopolymers* **1998**, *47*, 225−241.

(11) Ripka, W. C. Protein Tyrosine Phosphatase Inhibitors *Annu. Rep. Med. Chem.* **2000**, *35*, 231−250.

(12) Burke, T. R.; Kole, H. K.; Roller, P. P. Potent inhibition of insulin receptor dephosphorylation by a hexamer peptide containing the phosphotyrosyl mimetic F_2Pmp. *Biochem. Biophys. Res. Commun.* **1994**, *204*, 129−134.

(13) Chen, L.; Wu, L.; Otaka, A.; Smyth, M. S.; Roller, P. R.; Burke, T. R.; den Hertog, J.; Zhang, Z.-Y. Why is phosphonodifluoromethyl phenylalanine a more potent inhibitory moiety than phosphonomethyl phenylalanine toward protein-tyrosine phosphatases? *Biochem. Biophys. Res. Commun.* **1995**, *216*, 976−984.

(14) Moran, E. J.; Sarshar, S.; Cargill, J. F.; Shahbaz, M. M.; Lio, A.; Mjalli, A. M. M.; Armstrong, R. W. Radio frequency tag encoded combinatorial library method for the discovery of tripeptide-substituted cinnamic acid inhibitors of protein tyrosine phosphatases. *J. Am. Chem. Soc.* **1995**, *117*, 10787−10788.

(15) Liotta, A. S.; Kole, H. K.; Fales, H. M.; Roth, J.; Bernier, M. A synthetic tris-sulfotyrosyl dodecapeptide analogue of the insulin receptor 1146-kinase domain inhibits tyrosine dephosphorylation of the insulin receptor in situ. *J. Biol. Chem.* **1994**, *269*, 22996.

(16) Desmarais, S.; Jia, Z.; Ramachandran, C. Inhibition of protein tyrosine phosphatases PTP1B and CD45 by sulfotyrosyl peptides. *Arch. Biochem. Biophys.* **1998**, *345*, 225−231.

(17) Kole, H. K.; Akamatsu, M.; Ye, B.; Yan, X.; Barford, D.; Roller, P. P.; Burke, T. R. Protein-tyrosine phosphatase inhibition by a peptide containing the phosphotyrosyl mimetic, L-*O*-malonyltyrosine. *Biochem. Biophys. Res. Commun.* **1995**, *209*, 817−822.

(18) Burke, T. R.; Ye, B.; Akamatsu, M.; Ford, H.; Yan, X.; Kole, H. K.; Wolf, G.; Shoelson, S. E.; Roller, P. P. 4′-*O*-[2-(2-fluoromalonyl)]-L-tyrosine: a phosphotyrosyl mimic for the preparation of signal transduction inhibitory peptides. *J. Med. Chem.* **1996**, *39*, 1021−1027.

(19) Akamatsu, M.; Roller, P. P.; Chen, L.; Zhang, Z.-Y.; Ye, B.; Burke, T. R., Jr. Potent inhibition of protein-tyrosine phosphatase by phosphotyrosine-mimic containing cyclic peptides. *Bioorg. Med. Chem.* **1997**, *5*, 157−163.

(20) Gao, Y.; Wu, L.; Luo, J. H.; Guo, R.; Yang, D.; Zhang, Z.-Y.; Burke, T. R., Jr. Examination of novel non-phosphorus-containing phosphotyrosyl mimetics against protein-tyrosine phosphatase-1B and demonstration of differential affinities toward Grb2 SH2 domains. *Bioorg. Med. Chem. Lett.* **2000**, *10*, 923−927.

(21) Kole, H. K.; Smyth, M. S.; Russ, P. L.; Burke, T. R., Jr. Phosphonate inhibitors of protein-tyrosine and serine/threonine phosphatases. *Biochem. J.* **1995**, *311* (3), 1025−1031.

(22) Burke, T. R., Jr.; Ye, B.; Yan, X.; Wang, S.; Jia, Z.; Chen, L.; Zhang, Z.-Y.; Barford, D. Small molecule interactions with protein-tyrosine phosphatase PTP1B and their use in inhibitor design. *Biochemistry* **1996**, *35*, 15989−15986.

(23) Taylor, S. D.; Kotoris, C. C.; Dinaut, A. N.; Wang, Q.; Ramachandran, C.; Huang, Z. Potent non-peptidyl inhibitors of protein tyrosine phosphatase 1B. *Bioorg. Med. Chem.* **1998**, *6*, 1457−1468.

(24) Taylor, S. D.; Kotoris, C. C.; Dinaut, A. N.; Wang, Q.; Ramachandran, C.; Huang, Z. Potent non-peptidyl inhibitors of protein tyrosine phosphatase 1B (correction). *Bioorg. Med. Chem.* **1998**, *6*, 2235.

(25) Wang, Q.; Huang, Z.; Ramachandran, C.; Dinaut, A. N.; Taylor, S. D. Naphthalenebis[α,α-difluoromethylenephosphonates] as potent inhibitors of protein tyrosine phosphatases. *Bioorg. Med. Chem. Lett.* **1998**, *8*, 345−350.

(26) Rice, R. L.; Rusnak, J. M.; Yokokawa, F.; Yokokawa, S.; Messner, D. J.; Boynton, A. L.; Wipf, P.; Lazo, J. S. A targeted library of small-molecule, tyrosine, and dual-specificity phosphatase inhibitors derived from a rational core design and random side chain variation. *Biochemistry* **1997**, *36*, 15965−15974.

(27) Malamas, M. S.; Sredy, J.; Gunawan, I.; Mihan, B.; Sawicki, D. R.; Seestaller, L.; Sullivan, D.; Flam, B. R. New azolidinediones as inhibitors of protein tyrosine phosphatase 1B with antihyperglycemic properties. *J. Med. Chem.* **2000**, *43*, 995−1010.

(28) Malamas, M. S.; Sredy, J.; Moxham, C.; Katz, A.; Xu, W.; McDevitt, R.; Adebayo, F. O.; Sawicki, D. R.; Seestaller, L.; Sullivan, D.; Taylor, J. R. Novel benzofuran and benzothiophene biphenyls as inhibitors of protein tyrosine phosphatase 1b with antihyperglycemic properties. *J. Med. Chem.* **2000**, *43*, 1293−1310.

(29) Wrobel, J.; Sredy, J.; Moxham, C.; Dietrich, A.; Li, Z.; Sawicki, D. R.; Seestaller, L.; Wu, L.; Katz, A.; Sullivan, D.; Tio, C.; Zhang, Z.-Y. PTP1B inhibition and antihyperglycemic activity in the ob/ob mouse model of novel 11-arylbenzo[*b*]naphtho[2,3-d]furans and 11-arylbenzo[*b*]naphtho[2,3-d]thiophenes. *J. Med. Chem.* **1999**, *42*, 3199−3202.

(30) Iverson, L. F.; Anderson, H. S.; Branner, S.; Mortensen, S. B.; Peters, G. H.; Norris, K.; Olsen, O. H.; Jeppesen, C. B.; Lundt, B. F.; Ripka, W. B.; Moller, K. B.; Moller, N. P. H. Structure-based design of a low molecular weight, nonphosphorus, nonpeptide, and highly selective inhibitor of protein-tyrosine phosphatase 1B. *J. Biol. Chem.* **2000**, *275*, 10300−10307.

(31) Andersen, H. S.; Iversen, L. F.; Jeppesen, C. B.; Branner, S.; Norris, K.; Rasmussen, H. B.; Moller, K. B.; Moller, N. P. 2-(Oxalylamino)-benzoic acid is a general, competitive inhibitor of protein-tyrosine phosphatases. *J. Biol. Chem.* **2000**, *275*, 7101−7108.

(32) Puius, Y. A.; Zhao, Y.; Sullivan, M.; Lawrence, D. S.; Almo, S. C.; Zhang, Z. Y. Identification of a second aryl phosphate-binding site in protein-tyrosine phosphatase 1B: a paradigm for inhibitor design. *Proc. Natl. Acad. Sci. U.S.A.* **1997**, *94*, 13420−13425.

(33) Montserat, J.; Chen, L.; Lawrence, D. S.; Zhang, Z.-Y Potent low molecular weight substrates for protein-tyrosine phosphatase. *J. Biol. Chem.* **1996**, *271*, 7868−7872.

(34) Taing, M.; Keng, Y. F.; Shen, K.; Wu, L.; Lawrence, D. S.; Zhang, Z. Y. Potent and highly selective inhibitors of the protein tyrosine phosphatase 1B. *Biochemistry* **1999**, *38*, 3793−3803.

(35) Desmarais, S.; Friesen, R. W.; Zamboni, R.; Ramachandran, C. [Difluro(phosphono)methyl]phenylalanine-containing peptide inhibitors of protein tyrosine phosphatases. *Biochem. J.* **1999**, *337*, 219−223.

(36) Jia, Z.; Barford, D.; Flint, A. J.; Tonks, N. K. Structural basis for phosphotyrosine peptide recognition by protein tyrosine phosphatase 1B. *Science* **1995**, *268*, 1754−1758.

(37) Laskowski, R. A.; MacArthur, M. W.; Moss, D. S.; Thronton, J. M. PROCHECK: a program to check the stereochemical quality of protein structures. *J. Appl. Crystallogr.* **1993**, *27*, 283−291.

(38) Groves, M. R.; Yao, Z.-J.; Roller, P. P.; Burke, T. R.; Barford, D. Structural basis for inhibition of the protein tyrosine phosphatase 1B by phosphotyrosine peptide mimetics. *Biochemistry* **1998**, *37*, 17773.

(39) Yao, Z. J.; Ye, B.; Wu, X. W.; Wang, S.; Wu, L.; Zhang, Z. Y.; Burke, T. R., Jr. Structure-based design and synthesis of small molecule protein-tyrosine phosphatase 1B inhibitors. *Bioorg. Med. Chem.* **1998**, *6*, 1799−1810.

(40) Salmeen, A.; Anderson, J. N.; Myers, M. P.; Tonks, N. K.; Barford, D. Molecular basis for the dephosphorylation of the activation segment of the insulin receptor by protein tyrosine phosphatase 1B. *Mol. Cell* **2000**, *6*, 1401−1412.

(41) Ibarra-Sanchez, M. de J.; Simoncic, P. D.; Nestel, F. R.; Duplay, P.; Lapp, W. S.; Tremblay, M. L. The T-cell protein tyrosine phosphatase. *Semin. Immunol.* **2000**, *12*, 379−386.

(42) Walchli, S.; Curchod, M.-L.; Gobert, R. P.; Arkinstall, S.; Hooft van Huijsduuijnen, R. Identification of tyrosine phosphatases that dephosphorylate the insulin receptor. A brute force approach based on "substrate-trapping" mutants. *J. Biol. Chem.* **2000**, *275*, 9792−9796.

(43) You-Ten, K. E.; Muise, E. S.; Itie, A.; Michaliszyn, E.; Wagner, J.; Jothy, S.; Lapp, W. S.; Tremblay, M. L. Impaired bone marrow microenvironment and immune function in T cell protein tyrosine phosphatase-deficient mice. *J. Exp. Med*. **1997**, *186*, 683−693.
(44) Hooft van Huijsduuijnen, R. Protein tyrosine phosphatases: counting the trees in the forest. *Gene* **1998**, *225*, 1−8.
(45) Yang, J.; Liang, X.; Niu, T.; Meng, W.; Zhao, Z.; Zhou, G. W. Crystal Structure of the Catalytic Domain of Protein−Tyrosine Phosphatase SHP-1 *J. Biol. Chem*. **1998**, *273*, 28199−28207.
(46) Fauman, E. B.; Cogswell, J. P.; Lovejoy, B.; Rocque, W. J.; Holmes, W.; Montana, V. G.; Piwinica-Worms, H.; Rink, M. J.; Saper, M. A. Crystal structure of the catalytic domain of the human cell cycle control phosphatase, Cdc25A. *Cell* **1998**, *93*, 617−662.
(47) Burke, T. R.; Yao, Z.-J.; Liu, D.-G.; Voight, J.; Gao, Y. Phosphotyrosylmimetics in the Design of Peptide-Based Signal Transduction Inhibitors. *Biopolymers (Pept. Sci.)* **2001**, *60*, 32−44.
(48) Liu, S.; Dockendorf, C.; Taylor, S. D. Synthesis of protected L-4-[Sulfono(difluoromethyl)]phenylalanine and its incorporation into a peptide. *Org. Lett.* **2001**, *3*, 1571.
(49) Taylor, S. D.; Dinaut, A. N.; Thadani, A.; Huang, Z. Synthesis of Benzylic Mono(α,α-difluoromethylphosphonates) and Benzylic Bis(α,α-difluoromethylphosphonates) via Electrophilic Fluorination. *Tetrahedron Lett.* **1996**, *45*, 8089−8092.
(50) Taylor, S. D.; Kotoris, C. C.; Dinaut, A. N.; Chen, M.-J. Synthesis of Aryl(difluoromethylenephosphonates) via Electrophilic Fluorination of α-Carbanions of Benzylic Phosphonates with *N*-Fluorobenzenesulfonimide. *Tetrahedron* **1998**, *54*, 1691−1714.
(51) Huyer, G.; Liu, S.; Kelly, J.; Moffat, J.; Payette, P.; Kennedy, B.; Tsaprilis, G.; Gresser, M. J.; Ramachandran, C. Mechanism of inhibition of protein-tyrosine phosphatases by vanadate and pervanadate. *J. Biol. Chem*. **1997**, *272*, 843−851.
(52) Wang, Q.; Scheigetz, J.; Gilbert, M.; Snider, J.; Ramachandran, C. Fluorescein monophosphates as fluorogenic substrates for protein tyrosine phosphatases. *Biochim. Biophy. Acta* **1999**, *1431*, 14−23.
(53) Summers, M. D.; Smith, G. E. *A Manual for Methods for Baculovirus Vector and Insect Culture Procedures*; Bulletin No. 1555; Texas A & M University: Texas Agricultural Experiment Station, College Station, TX, 1987.
(54) Barford, D.; Keller, J. C.; Flint, A. J.; Tonks, N. K. Purification and crystallization of the catalytic domain of human protein tyrosine phosphatase 1B expressed in *Escherichia coli*. *J. Mol. Biol.* **1994**, *239*, 726−730.
(55) Otwinowski, Z.; Minor, W. Processing of X-ray diffraction data collected in oscillation mode. *Methods Enzymol.* **1997**, *276*, 307−326.
(56) Kissinger, C. R.; Gehlhaar, D. K. EPMR: A program for crystallographic molecular replacement by evolutionary search, October 1997.
(57) Brünger, A. T.; Adams, P. D.; Clore, G. M.; DeLano, W. L.; Gros, P.; Grosse-Kunstleve, R. W.; Jiang, J. S.; Kuszewski, J.; Nilges, M.; Pannu, N. S.; Read, R. J.; Rice, L. M.; Simonson, T.; Warren, G. L. Crystallography and NMR system: a new software system for macromolecular structure determination. *Acta Crystallogr*. **1998**, *D54*, 905−921.
(58) McRee, D. E. A visual protein crystallographic software system for X11/XView. *J. Mol. Graphics* **1992**, *10*, 44−46.
(59) Kraulis, P. J. MOLSCRIPT: a program to produce both detailed and schematic plots of protein structures. *J. Appl. Crystallogr*. **1991**, 24, 946−950.
(60) Merritt, E. A.; Bacon, D. J. Raster3D: Photorealisticmolecular graphics. *Methods Enzymol*. **1997** *277*, 505−524.

JM010266W